Monografías del Seminario Matemático García de Galdeano **33**, 349–356 (2006)

A NUMERICAL METHOD FOR SIMULATING TURBULENT SHEAR FLOWS WITH LOW REYNOLDS $k-\varepsilon$ MODELS

Y. Bentaleb, E. Schall, B. Koobus, A. Dervieux and M. Amara

Abstract. We present a new numerical model for the simulation of turbulent flows. New numerics rely on a 3D upwind compressible solver which applies to (possibly unstructured) tetrahedrizations. Accuracy in boundary layers is increased by a new type of tetrahedrization. The Reynolds-Averaged Navier-Stokes (RANS) equations are solved using a mixed element-volume method for the spatial discretization and an implicit scheme is applied to advance the equations in time. Two low Reynolds number $k-\varepsilon$ RANS models are implemented with this numerical technique. A linear model, the low Reynolds number $k-\varepsilon$ turbulence model of Goldberg *et al.*, and a nonlinear one using a cubic relation between the strain and vorticity tensors and the stress tensor, as originally proposed by Craft *et al.* These models are applied to the study of a turbulent flow past a backward-facing step. The results obtained are compared to experimental data.

Keywords: Low Reynolds turbulence modeling, linear and nonlinear $k-\varepsilon$, mixed element-volume method.

§1. Introduction

The prediction of complex three-dimensional turbulent shear flows remains a grand challenge for computational fluid dynamics (CFD). Such flows take place over simple to complex 3D geometries for many practical situations. A new family of tools are studied for the prediction of such flows. The ingredients are: (i) low dissipation numerics applying to unstructured meshes, (ii) statistical turbulence modeling, typically of Reynolds Average Navier-Stokes (RANS) type, (iii) hybridisation with Large Eddy Simulation (LES).

This paper focuses on (i) and (ii), but with the perspective of improving type (iii) approaches. Indeed we start from a numerical methodology which already applies to type (iii). In [1], an implicit mixed-element-volume numerical method applying to unstructured meshes and able to predict compressible and incompressible flows is associated with an hybridisation of a LES model and a high Reynolds linear $k-\varepsilon$. In this paper, we consider the same numerical techniques as in [1] and introduce two kinds of improvements, a numerical treatment of thin boundary layers, and two low Reynolds RANS models. Three specific requirements for selecting the turbulence closure are accounted for: (a) it should be the best possible model to predict complex turbulent flows of practical interest; (b) it must be wall-distance-free, thus applicable to complex 3D geometries in conjunction with unstructured grid based solver; (c) it should represent correctly normal stresses anisotropy. For (c) we consider a nonlinear

stress-strain relation. This relation goes back at least to the proposal of Pope [2]. The introduction of nonlinear terms up to cubic level makes the Reynolds stresses a more general function of mean velocities and vorticities [3]. In this work, the turbulence closure models for RANS equations used in the computations are the linear low Reynolds $k-\varepsilon$ model proposed by Goldberg *et al.* [4] and a nonlinear extension formulated by Batten *et al.* [5]. Preliminary experiments on a turbulent flow past a backward-facing step are presented. After Section 2 in which the turbulence models under study are described, we devote Section 3 to the numerical standpoint. Section 4 is a discussion of numerical experiments. Some concluding remarks are given in Section 5.

§2. Eddy-viscosity models for Reynolds stresses

2.1. Low-Reynolds number $k-\varepsilon$ model

In order to model accurately the turbulent flow down to the wall, a standard $k-\varepsilon$ model must be locally adapted according to parameters indicating the grid point position in a possible boundary layer. For complex geometries these parameters must be as much wall distance free as possible. Goldberg *et al.* proposed in [4] a low Reynolds number extension designed to improve prediction of adverse pressure gradient flows, including separated and reattaching flows. In addition, the model, compared with the other low Reynolds models proposed in the literature, has the advantage to be wall-distance-free, it also invokes a simple boundary condition for ε. Transport equations for k and ε write:

$$\frac{\partial \bar{\rho}\tilde{k}}{\partial t}+\frac{\partial (\bar{\rho}\tilde{u}_i\tilde{k})}{\partial x_i}=\frac{\partial}{\partial x_i}\left[\left(\mu+\frac{\mu_t}{\sigma_k}\right)\frac{\partial \tilde{k}}{\partial x_i}\right]+\mathscr{P}_k-\bar{\rho}\tilde{\varepsilon}, \tag{1}$$

$$\frac{\partial \bar{\rho}\tilde{\varepsilon}}{\partial t}+\frac{\partial (\bar{\rho}\tilde{u}_i\tilde{\varepsilon})}{\partial x_i}=\frac{\partial}{\partial x_i}\left[\left(\mu+\frac{\mu_t}{\sigma_\varepsilon}\right)\frac{\partial \tilde{\varepsilon}}{\partial x_i}\right]+(C_{\varepsilon 1}\,\mathscr{P}_k-C_{\varepsilon 2}\,\bar{\rho}\tilde{\varepsilon}+E)\;T_t^{-1}, \tag{2}$$

with E being the extra source term and T_t the realizable time scale :

$$E=A_E\bar{\rho}\mathscr{V}\sqrt{\tilde{\varepsilon}T_t}\,\Psi,\quad \Psi=\max\left\{\frac{\partial\tilde{k}}{\partial x_i}\frac{\partial\tau}{\partial x_i},0\right\},\quad \mathscr{V}=\max\left\{\tilde{k}^{1/2},(\nu\tilde{\varepsilon})^{1/4}\right\},$$

$$T_t=\frac{\tilde{k}}{\tilde{\varepsilon}}\max\left\{1,\xi^{-1}\right\},\quad \xi\equiv\sqrt{R_t}/C_\tau,\quad R_t\equiv\tilde{k}^2/(\nu\tilde{\varepsilon}),\quad C_\tau=\sqrt{2},\quad A_E=0.3,$$

where $\tau=\tilde{k}/\tilde{\varepsilon}$ is the turbulence time scale. The eddy-viscosity μ_t is defined with a damping function f_μ in order to enable a correct behavior in near-wall regions.

$$\mu_t=f_\mu C_\mu\frac{\bar{\rho}\tilde{k}^2}{\tilde{\varepsilon}},\quad f_\mu=\frac{1-e^{-0.01R_t}}{1-e^{-\sqrt{R_t}}}\max\left\{1,\xi^{-1}\right\},\quad C_{\varepsilon 1}=1.44,\quad C_{\varepsilon 2}=1.92\,.$$

The boundary conditions have a crucial influence on the quality of practical simulations. For the turbulent quantities, they are defined as $\tilde{k}_w=0$ and $\tilde{\varepsilon}_w=2\nu_1\tilde{k}_1/y_1^2$ where "1" denotes the centroid of the first cell away from walls. There is no ambiguity in the definition of y_1, compared to low Reynolds models which involve explicit wall distance in the entire domain. In this regard, the model preserves the wall-distance-free attribute.

2.2. Nonlinear stress-strain relationship

In the class of linear Eddy-Viscosity Models (EVM), the Reynolds stresses are expressed in terms of the mean strain rate (Boussinesq assumption), in the same way as the viscous stress for Newtonian isotropic fluid, through the use of an isotropic eddy viscosity in place of the molecular viscosity. Several deficiencies in the prediction of the turbulence quantities are attributed to these models, including streamline curvature effects, misrepresentation of the normal stresses (predicted as isotropic), and inability to capture the secondary flows.

A nonlinear formulation of the previous model is proposed by Batten *et al.* [5], which assumes that the Reynolds stresses are a general function of mean velocities and vorticities [3]:

$$\begin{aligned}
\overline{\rho}\,\widetilde{u_i'' u_j''} = {} & \frac{2}{3}\overline{\rho}\tilde{k}\delta_{ij} - \mu_t \tilde{S}_{ij} \qquad \Longleftarrow \qquad \text{linear model} \\
& + c_1\,\mu_t \frac{\tilde{k}}{\tilde{\varepsilon}}\left(\tilde{S}_{ik}\tilde{S}_{kj} - \frac{1}{3}\tilde{S}_{kl}\tilde{S}_{kl}\delta_{ij}\right) + c_2\,\mu_t \frac{\tilde{k}}{\tilde{\varepsilon}}\left(\tilde{\Omega}_{ik}\tilde{S}_{kj} + \tilde{\Omega}_{jk}\tilde{S}_{ki}\right) \\
& + c_3\,\mu_t \frac{\tilde{k}}{\tilde{\varepsilon}}\left(\tilde{\Omega}_{ik}\tilde{\Omega}_{jk} - \frac{1}{3}\tilde{\Omega}_{kl}\tilde{\Omega}_{kl}\delta_{ij}\right) + c_4\,\mu_t \frac{\tilde{k}^2}{\tilde{\varepsilon}^2}\left(\tilde{S}_{ki}\tilde{\Omega}_{lj} + \tilde{S}_{kj}\tilde{\Omega}_{li}\right)\tilde{S}_{kl} \qquad (3) \\
& + c_5\,\mu_t \frac{\tilde{k}^2}{\tilde{\varepsilon}^2}\left(\tilde{\Omega}_{il}\tilde{\Omega}_{lm}\tilde{S}_{mj} + \tilde{S}_{il}\tilde{\Omega}_{lm}\tilde{\Omega}_{mj} - \frac{2}{3}\tilde{S}_{lm}\tilde{\Omega}_{mn}\tilde{\Omega}_{nl}\delta_{ij}\right) \\
& + c_6\,\mu_t \frac{\tilde{k}^2}{\tilde{\varepsilon}^2}\tilde{S}_{ij}\tilde{S}_{kl}\tilde{S}_{kl} + c_7\,\mu_t \frac{\tilde{k}^2}{\tilde{\varepsilon}^2}\tilde{S}_{ij}\tilde{\Omega}_{kl}\tilde{\Omega}_{kl},
\end{aligned}$$

with $\tilde{S}_{ij} = \dfrac{\partial \tilde{u}_i}{\partial x_j} + \dfrac{\partial \tilde{u}_j}{\partial x_i} - \dfrac{2}{3}\dfrac{\partial \tilde{u}_k}{\partial x_k}\delta_{ij}$ and $\tilde{\Omega}_{ij} = \dfrac{\partial \tilde{u}_i}{\partial x_j} - \dfrac{\partial \tilde{u}_j}{\partial x_i}$ are the mean strain tensor and mean rotation tensor, respectively. The constants of the model can be found in [5].

§3. Numerical methodology

One of the important purposes of the present study is the increase of accuracy in highly stretched boundary layers for a numerical technology which applies to tetrahedrizations.

By highly stretched boundary layer, we mean a flow region limited by a wall where mesh stretching needs to be as high as tens of thousands.

Variational methods applying to general (possibly unstructured) tetrahedrizations have a convergence theory well established for basic models thanks, in particular, to hilbertian analysis, but extension to nonlinearities, especially when they involve spatial derivatives of unknowns is delicate. This is why, in today's state of the art, numerical approximations for highly stretched boundary layers use quasi-cartesian meshes on those regions, in order to enjoy finite-difference convergence mechanisms (uniform convergence of unknowns and derivatives). In order to realize this program for tetrahedra, we have adapted to boundary layers a method introduced by Gourvitch *et al.* [6]. In their paper, these authors were looking for high order accurate (up to sixth-order) schemes for acoustics. They manage to get a numerical tetrahedrization-based scheme which reduces to the usual finite volume method on cubes for a particular tetrahedrization. The central idea is to split cubes into six orthogonal tetrahedra. By orthogonal tetrahedron we mean a tetrahedron such that three edges are orthogonal

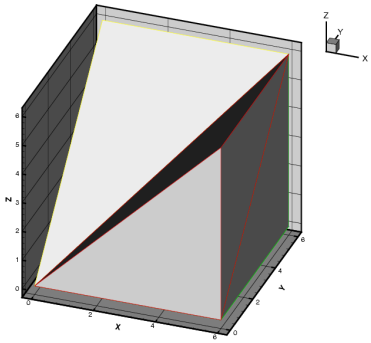

Figure 1: Splitting of a cube in orthogonal tetrahedra: view of the cube after two tetrahedra have been taken off [6].

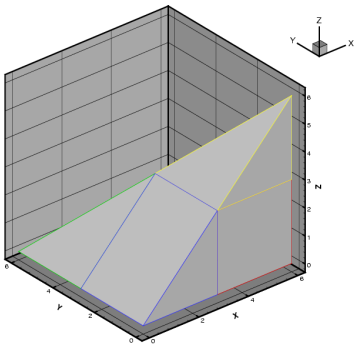

Figure 2: Construction of dual cells for an orthogonal tetrahedron.

to each other (see Fig.1). This splitting is completed by a particular decomposition of the tetrahedrization in dual control volumes introduced in [7] which relies on the center of the smallest sphere containing the tetrahedron (see Fig.2). The proposed improvement consists in using in the boundary layer a mesh relying on parallelepipeds split into orthogonal tetrahedra and to apply the above dual cell construction. This improvement is introduced in a *mixed finite-volume finite-element approximation* [8] solving the compressible Euler equations. The convective fluxes use Roe's flux splitting with Turkel's low Mach preconditioner and produce accurate approximation of incompressible flow as far as a Mach number less than 0.1 is specified. For what concerns the time-advancing procedure, a fully implicit scheme is employed. The time discretization is based on a second-order backward difference scheme. The nonlinear flow equations derived from the time-discretization are solved by a defect-correction (Newton-like) method [9].

§4. Test case : The backward-facing step

We consider an incompressible flow over a three-dimensional backward-facing step, measured experimentally by Driver and Seegmiller [10]. This flow has been studied by many authors and we refer to the recent state of art paper of Kim *et al.* [11]. The Reynolds number based on the step height H is equal to 37422, and the freestream Mach number to 0.1. The computational domain extends from $-4H$ upstream (*inlet*) to $32H$ downstream (*outlet*) from the step which is located at $x = 0$. The grid is composed of two parts which contain $(35 \times 101 \times 3)$ and $(221 \times 161 \times 3)$ nodes respectively, 51 points are used in the recirculation region downstream of the step, and the grid is clustered in the y direction near walls (Fig. 3). Separate one-dimensional finite element code, which resolves a turbulent channel flow case, was preliminary validated by the Comte-Bellot experimental data [12] and used to specify the inflow and outflow. It uses the reference velocity and experimental skin friction velocity. Dirichlet conditions are applied at the upstream boundary, and the numerical flux splitting of Steger-Warming is used at outflow where the far-field part is obtained with these separate

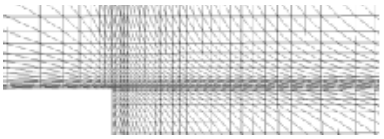

Figure 3: Reduced-aspect ratio cells near the step corner.

calculations. No-slip conditions are imposed on the walls, and slip conditions are applied to the lateral side of the computational domain. The computation is considered to be converged when the normalized residual of total energy was less than 0.05%.

4.1. Some results

The RANS closure models used for the backward-facing step computations which are presented hereafter were preliminary validated with the turbulent channel flow case experimented by Comte-Bellot [12]. In Figs. 4 and 5 are depicted the streamwise velocity and Reynolds shear stress predictions which show overall satisfactory results. The so-called "1D profile" represents the separate one-dimensional calculation.

For the backward-facing step mesh, the computed values of y^+ along the step-side wall reported in Fig. 6 shows that the first off-wall grid point is always located below $y^+ = 1$. The inlet streamwise velocity profiles are depicted in Fig. 7. Lower wall static pressure and skin-friction coefficients are presented in Figs. 8 and 9. The C_p is well predicted in the recirculation region with the nonlinear model, while the linear one fails in the correct restitution of the negative peak. However both models overpredict the C_p downstream the reattachment point. A good qualitative job is obtained in the C_f prediction, although the level is underpredicted in the separated region. This is consistent with many results obtained in other works for different $k-\varepsilon$ models. The reattachment length is presented in the literature as a critical parameter to assess the performance of a turbulent simulation for this test-case. Many CFD results based on eddy-viscosity models have reported a reattachment that occurs up to 30% upstream than measurements. In our calculations, satisfactory results are obtained. The predicted reattachment lengths as well as the experimental one are listed in table 1. The linear model overpredicts the reattachment length by 5.7%, while nonlinear model prediction is within 2.2% of the measurement. In this regard, the nonlinear model shows better performance than the linear one. As far as the turbulence anisotropy is concerned, Figs. 10 and 11 show that near the wall at $x/H = 4$, the linear model gives unrealistic results since $\widetilde{v''v''} > \widetilde{u''u''}$. As expected, the nonlinear model recovers at least the qualitatively correct behavior of the normal Reynolds stresses.

Model	Linear model [4]	Nonlinear model [5]	Experiment [10]
Reattachment point (x/H)	6.62	6.40	6.26

Table 1: Predicted and experimental reattachment point.

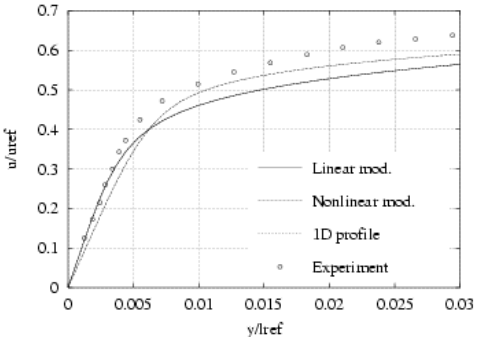

Figure 4: Streamwise velocity profiles in turbulent channel flow. $u_{ref} = 10.5\,m/s$.

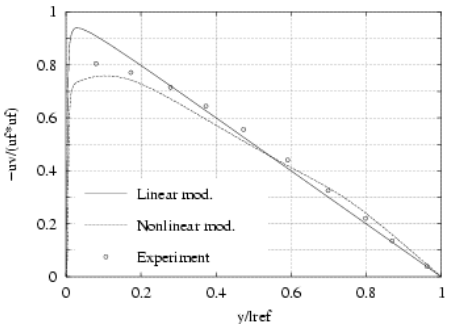

Figure 5: Reynolds shear stress profiles in turbulent channel flow. $u_\tau = 0.39\,m/s$.

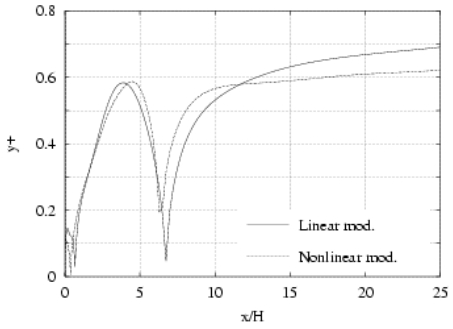

Figure 6: Distribution of y^+ along the step-side wall.

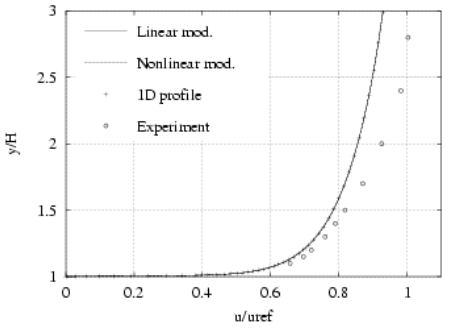

Figure 7: Streamwise velocity profiles at $x/H = -4$, $u_{ref} = 44.2\,m/s$.

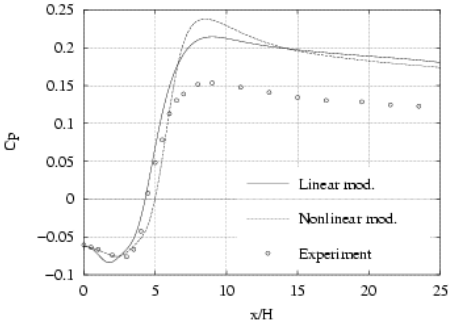

Figure 8: Wall static pressure distribution along the step-side wall. $C_p = \frac{2(\overline{p}-p_{ref})}{\rho_{ref}u_{ref}^2}$.

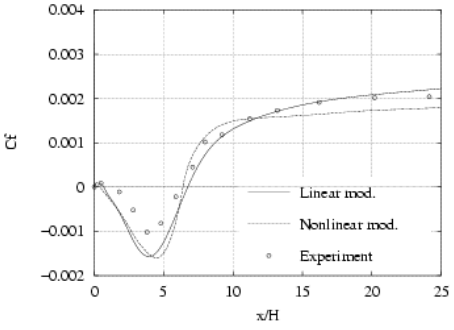

Figure 9: Skin-friction distribution along the step-side wall. $C_f = 2\tau_w/\rho_{ref}u_{ref}^2$.

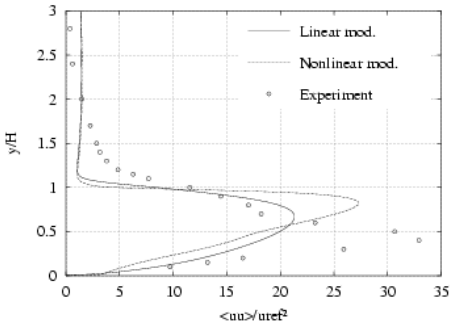

Figure 10: Normal Reynolds stress $\widetilde{u''u''}$ at $x/H = 4$.

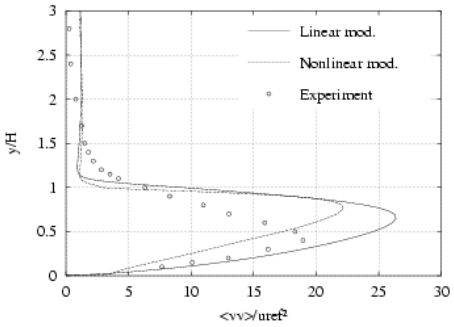

Figure 11: Normal Reynolds stress $\widetilde{v''v''}$ at $x/H = 4$.

§5. Conclusions

A Reynolds-Averaged Navier-Stokes numerical model based on a mixed element-volume formulation for unstructured meshes is extended to low Reynolds formulation and evaluated on a recirculating flow. A particular tetrahedrization is combined with a specific dual cell partition in order to increase thin boundary layer resolution. The new model exhibits promising capability in predicting near-wall turbulent flows with good accuracy. The results show an overall good agreement with the experimental data, particularly for the skin-friction distribution and reattachment point predictions, with global better predictions for the non-linear eddy viscosity model, specially when normal Reynolds stresses are considered. Further developments and tests will be carried out to improve the predictions for different flow configurations.

Acknowledgements

This work was supported by the Conseil Régional d'Aquitaine. The authors thank the Centre Informatique National de l'Enseignement Supérieur (CINES) for providing the computational resources.

References

[1] CAMARRI, S., SALVETTI, M.V., KOOBUS, B., AND DERVIEUX, A. Bluff-body flow simulation by an hybrid RANS/LES approach. *Wing and Structures. 8*, 6 (2005), 407–426.

[2] POPE, S. B. A more general effective viscosity hypothesis. *Journal of Fluid Mechanics 72* (1975), 331–340.

[3] CRAFT, T. J., LAUNDER, B. E., AND SUGA, K. Development and application of a cubic Eddy-viscosity model of turbulence. *Int. J. Heat and Fluid Flow 17* (1996), 108–115.

[4] GOLDBERG, U., PEROOMIAN, O., AND CHAKRAVARTHY, S. A wall-distance-free $k-\varepsilon$ model with enhanced near-wall treatment. *J. Fluids Engrg. 120* (1998), 457–462.

[5] BATTEN, P., GOLDBERG, U., AND CHAKRAVARTHY, S. Sub-grid turbulence modeling for unsteady flow with acoustic resonance. *AIAA-00-0473* (2000).

[6] GOURVITCH, N., ROGÉ, G., ABALAKIN, I., DERVIEUX, A., AND KOZUBSKAYA, T. A tetrahedral-based superconvergent scheme for aeroacoustics. *Research Report INRIA* no. 5212 (2004).

[7] BARTH, T. Aspects of unstructured grids and finite-volume solvers for the Euler and Navier-Stokes equations. In *Special Course on Unstructured Grid Methods for Advection Dominated Flows*, AGARD report 787 (1992), 6-1 to 6-61.

[8] DERVIEUX, A.. Steady Euler simulations using unstructured meshes. *Von Karman Institute for Fluid Dynamics, Lecture Series 1985-04.* Comput. Fluid Dynamics (1985).

[9] MARTIN, R., AND GUILLARD, H. A second order defect correction scheme for unsteady problems. *Computer and Fluids 25* (1996) 9–27.

[10] DRIVER, D. M., AND SEEGMILLER, H. L. Features of a reattaching turbulent shear layer in divergent channel flow. *AIAA Journal 23*, 2 (1985), 163–171.

[11] KIM, J. Y., GHAJAR, A. J., TANG, C., AND FOUTCH, G. L. Comparison of near-wall treatment methods for high Reynolds numbrer backward-facing step flow. *Int. J. of Computational Fluid Dynamics 19*, 7 (2005), 493–500.

[12] COMTE-BELLOT, G. Contribution à l'étude de la turbulence de conduite. *Thèse de Docteur ès Sciences*, Université de Grenoble, 1963.

Yacine Bentaleb and Eric Schall
Laboratoire de Thermique, Energétique et Procédés, EA 1932
Université de Pau et des Pays de l'Adour. 1, avenue de l'Université 64000 Pau, France
yacine.bentaleb@etud.univ-pau.fr and eric.schall@univ-pau.fr

Bruno Koobus
Laboratoire d'Analyse, Calcul Scientifique et Optimisation de Montpellier, FRE 2311 CNRS
Université de Montpellier II. Département de Mathématiques, Case Courrier 51
34095 Montpellier Cedex 5, France. koobus@darboux.math.univ-montp2.fr

Alain Dervieux
Institut National de Recherche en Informatique et en Automatique
INRIA, 2003 Route des Lucioles F-06902 Sophia-Antipolis Cedex, France
alain.dervieux@inria.fr

Mohamed Amara
Laboratoire de Mathématiques Appliquées
CNRS UMR 5142 - Université de Pau et des Pays de l'Adour
IPRA, B.P. 1155, 64013 Pau Cedex, France
mohamed.amara@univ-pau.fr